

LBL--30989

DE92 017114

**FORMATION OF BURIED EPITAXIAL Si-Ge ALLOY LAYERS IN  
Si <100> CRYSTAL BY HIGH DOSE Ge ION IMPLANTATION**

Kin Man Yu\*, Ian G. Brown \*\*, and Seongil Im\*\*\*

\*Center for Advanced Materials  
Materials Sciences Division  
and

\*\*Accelerator & Fusion Research Division  
Lawrence Berkeley Laboratory  
1 Cyclotron Road  
Berkeley, CA 94720

\*\*\*Materials Science and Mineral Engineering Department  
University of California at Berkeley  
Berkeley, CA 94720

Presented at the Fall 1991 Meeting of the Materials Research Society  
Boston, Dec. 2-6, 1991

This work was supported by the Director, Office of Energy Research, Office of Basic Energy Sciences, Materials Sciences Division of the U.S. Department of Energy under Contract No. DE-AC03-76SF00098.

MASTER  
DISTRIBUTION OF THIS DOCUMENT IS UNLIMITED

# FORMATION OF BURIED EPITAXIAL Si-Ge ALLOY LAYERS IN Si <100> CRYSTAL BY HIGH DOSE Ge ION IMPLANTATION

Kin Man Yu\*, Ian G. Brown\*\* and Seongil Im\*\*\*

\*Center for Advanced Materials, Materials Sciences Division and \*\*Accelerator & Fusion Research Division, Lawrence Berkeley Laboratory, Berkeley, CA 94720

\*\*\*Department of Materials Science and Mineral Engineering, University of California, Berkeley, CA 94720.

## ABSTRACT

We have synthesized single crystal  $Si_{1-x}Ge_x$  alloy layers in Si <100> crystals by high dose Ge ion implantation and solid phase epitaxy. The implantation was performed using the metal vapor vacuum arc (Mevva) ion source. Ge ions at mean energies of 70 and 100 keV and with doses ranging from  $1 \times 10^{16}$  to  $7 \times 10^{16}$  ions/cm<sup>2</sup> were implanted into Si <100> crystals at room temperature, resulting in the formation of  $Si_{1-x}Ge_x$  alloy layers with peak Ge concentrations of 4 to 13 atomic %. Epitaxial regrowth of the amorphous layers was initiated by thermal annealing at temperatures higher than 500°C. The solid phase epitaxy process, the crystal quality, microstructures, interface morphology and defect structures were characterized by ion channeling and transmission electron microscopy. Compositinally graded single crystal  $Si_{1-x}Ge_x$  layers with full width at half maximum ~100nm were formed under a ~30nm Si layer after annealing at 600°C for 15 min. A high density of defects was found in the layers as well as in the substrate Si just below the original amorphous/crystalline interface. The concentration of these defects was significantly reduced after annealing at 900°C. The kinetics of the regrowth process, the crystalline quality of the alloy layers, the annealing characteristics of the defects, and the strains due to the lattice mismatch between the alloy and the substrate are discussed.

## INTRODUCTION

In recent years, there has been much interest in the alloys of silicon and germanium,  $Si_{1-x}Ge_x$ , which have been shown to be promising semiconductor materials for the fabrication of high speed modulation-doped field effect transistors[1] and heterojunction bipolar transistors[2]. In addition to novel device applications,  $Si_{1-x}Ge_x$  alloy layers have been used as buffer layers for the growth of Si-Ge strained layer superlattices with novel optical properties. Conventionally defect-free and atomically abrupt  $Si_{1-x}Ge_x$  alloy thin films with x ranging from 0-50% can be grown on Si substrates by molecular beam epitaxy (MBE)[3], limited-reaction-processing (LRP) [4], and ion beam sputter deposition [5] techniques provided the layers are below the critical thickness for pseudomorphic growth [6,7]. Recently, the growth of  $Si_{1-x}Ge_x$  alloy layers, in particular buried  $Si_{1-x}Ge_x$  layers in Si, using ion beam synthesis (IBS) methods has also been explored [8-11].

In the last few years the IBS technique has been developed and applied to the synthesis of metal silicides in Si. Buried  $CoSi_2$ [12-16],  $NiSi_2$  [17,18],  $IrSi_3$  [19],  $CrSi_2$  [13,20],  $YSi_{1.7}$  [21],  $FeSi_2$  [20], etc. have been successfully fabricated by directly implanting energetic metal ions into Si. Using the IBS technique, White *et. al.* [13] have synthesized buried epitaxial  $CoSi_2$  layers which have electrical properties comparable to those grown by MBE. Despite the initial gaussian distribution of the implanted ions, subsequent annealing of the structure at temperatures  $\geq 500^\circ C$  resulted in good layer confinement in the buried silicide structures. The migration of the implanted ions from the tails of the profile towards the center is a result of the existence of a stable silicide phase in the metal-silicon phase diagram. In the case of the Si-Ge system, no such stable phase exists. In fact, Ge atoms are completely miscible in the Si lattice. Therefore when Ge ions are implanted into Si, no significant redistribution of the Ge atoms in the solid state is expected after annealing.

Recently, several investigators have explored the formation of  $Si_{1-x}Ge_x$  layers by IBS. Paine *et. al.* [8,9,11] have studied the IBS of  $Si_{1-x}Ge_x$  using transmission electron microscopy (TEM) and developed a model for the strain relief in compositionally graded SiGe layers. Berti *et. al.*[10] studied the formation of  $Si_{1-x}Ge_x$  layer by Ge implantation and laser melting. They found that the Ge atoms redistributed to the surface forming a sharp, epitaxial, defect-free  $Si_{1-x}Ge_x$  surface layer after irradiation by a  $XeCl$  laser at  $1.07 J/cm^2$ . In our work, we present a study of the formation of buried  $Si_{1-x}Ge_x$  epitaxial layers by IBS using a high current metal vapor

vacuum arc (Mevva) ion source. Issues on the solid phase epitaxial regrowth, crystalline quality and coherence of the  $\text{Si}_{1-x}\text{Ge}_x$  layers, as well as the recovery of the implanted damage are discussed.

## EXPERIMENTAL DETAILS

(100) oriented Si wafers were implanted with Ge ions at three different doses,  $1 \times 10^{16}$ ,  $1.7 \times 10^{16}$ , and  $7.0 \times 10^{16}/\text{cm}^2$  using the Mevva ion source. The three different doses will be referred to as low, medium and high dose, respectively in this paper. The details of the implantation set-up have been described in previous publications[19,22] and will not be repeated here. The substrate was water-cooled during implantation. The extraction voltage of the low dose implant was 50 kV while that of the medium and high dose implants was 70 kV. The mean charge state for the Ge ions produced by the ion source was  $\sim 1.4$  (60%  $\text{Ge}^+$  and 40%  $\text{Ge}^{++}$ ) [23]; since no energy analysis was carried out (broad-beam implantation), the mean implantation energy of the low dose implant was  $\sim 70$  keV and the mean energy of the medium and high dose implants was 100 keV. The Ge ions were implanted into the Si wafers with  $250 \mu\text{s}$  beam pulses at a maximum beam current of  $5\text{mA}/\text{cm}^2$ . The beam pulse repetition rate was limited to 3-5 pulses/second to avoid beam heating. After implantation, the samples were annealed in the temperature range of  $500\text{-}900^\circ\text{C}$  in a  $\text{N}_2$  ambient with the surface protected by a bare Si wafer.

The implanted Ge profiles were measured by Rutherford backscattering spectrometry (RBS) with a 1.95 MeV He ion beam. The RBS experiments were performed at scattering angle  $\theta=165^\circ$ . The solid phase epitaxial regrowth kinetics, the epitaxial quality of the  $\text{Si}_{1-x}\text{Ge}_x$  layers and the implantation damage were accessed by ion channeling in the  $\langle 100 \rangle$ ,  $\langle 110 \rangle$ ,  $\langle 111 \rangle$  axial directions. TEM of cross-sectional specimens was also carried out on some of the samples using the JEOL 200CX TEM at the National Center for Electron Microscopy at the Lawrence Berkeley Laboratory.

## RESULTS AND DISCUSSION

### I. Solid Phase Epitaxy (SPE)

Figure 1 shows the Ge atomic profiles for the three implants as measured by RBS. The peak Ge concentrations for the three doses correspond to 4 (low), 3.5 (medium), and 12.5 (high) atomic % while their projected ranges are 35nm, 55nm and 60nm, respectively. Note that the peak Ge concentration of the low dose sample is slightly higher than that of the medium dose sample. This is due to the higher implant energy of the medium dose implant which results in a wider spread in the Ge distribution and lower peak concentration. The calculated ranges using the

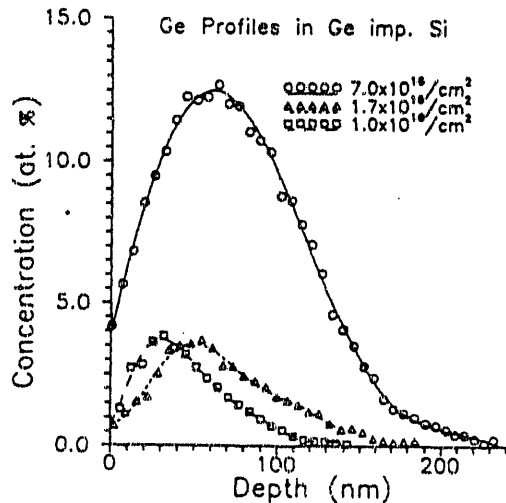


Fig. 1 The Ge atomic profiles in Si for the three different doses measured by RBS.

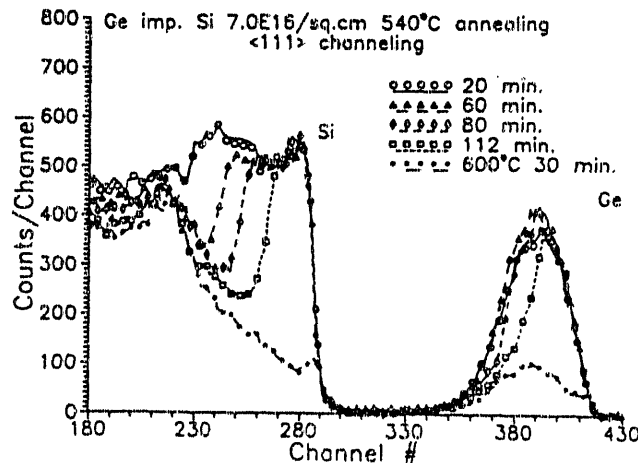


Fig. 2. A series of  $\langle 111 \rangle$  channelled RBS spectra from the high dose sample annealed at  $540^\circ\text{C}$  for various time durations.

LSS theory for 70 keV and 100 keV Ge ions in a Si crystal are 44 nm and 59 nm. These theoretical values agree reasonably well with the experimental values measured by RBS. The broad Ge distributions in Fig. 1 are the results of the multiple charge states of the Ge ions from the Mevva ion source [23]. Ion channeling measurements show that for the as-implanted samples, the amorphous layer thicknesses are 145 nm for the low dose, 170 nm for the medium dose, and 210 nm for the high dose cases.

Solid phase epitaxial (SPE) regrowth kinetics were studied by ion channeling techniques for both the low dose and the high dose samples. SPE is observed at annealing temperatures higher than 500°C. Fig. 2 shows a series of RBS spectra taken in the <111> channeling direction from the high dose sample annealed at 540°C for 20, 60, 80, and 112 min. The RBS spectrum from a fully regrown sample (600°C for 30 min.) is also included for comparison. Note that the regrowth proceeds in a planar fashion with sharp amorphous/crystalline (a/c) interfaces (to within 90 Å). A cross-sectional TEM micrograph of a partially regrown high dose sample (570°C for 25 min.) shown in Fig. 4 (a) confirms the uniform planar a/c interface during SPE. The data in Fig. 2 also shows that the SPE process is a linear function of the annealing time with a regrowth rate of  $\approx 1.3$  nm/min. at 540°C. Arrhenius plots of regrowth rate versus annealing temperature reveal that the activation energy for the SPE process,  $\Delta E = 2.5 \pm 0.2$  eV for the low dose sample and  $\Delta E = 3.0 \pm 0.2$  eV for the high dose case. The activation energy for the low dose sample is very similar to that of SPE Si ( $\Delta E = 2.6$  eV) [24] while the activation energy for the high dose case is significantly higher. This result is in good agreement with the SPE results of Paine et al. [25] who found that for  $\text{Si}_{1-x}\text{Ge}_x$  layers grown by UHV-CVD process and amorphized by Si implantation, the SPE regrowth rate is lower in the Si-Ge alloy layer than in pure Si with an activation energy  $= 3.2 \pm 0.2$  eV. However, in our experiment the change in the epitaxial regrowth rate as the crystallization front approaches regions with higher Ge concentration is not detectable due to the fact that the original amorphous layer is compositionally graded and the limited resolution of the RBS technique.

## II. Crystalline Quality of the $\text{Si}_{1-x}\text{Ge}_x$ layer

The quality of the  $\text{Si}_{1-x}\text{Ge}_x$  layers after SPE is measured by ion channeling along the <110> and <111> axes of the Si substrate. Fig. 3 shows the Ge signals from the random and <110> aligned RBS spectra of the (a) low and (b) high dose samples annealed at various conditions after SPE. A minimum yield for the Ge signal  $\chi_{\min}(\text{Ge}) = 4\%$  is achieved for the low dose sample just after SPE (600°C for 10 min). This is comparable to an unimplanted single crystal Si ( $\chi_{\min} \approx 3\%$ ). The low  $\chi_{\min}(\text{Ge})$  in this sample indicates that the  $\text{Si}_{1-x}\text{Ge}_x$  layer is a high quality single crystal. Cross sectional TEM on this sample reveals that the layer is indeed defect-free. Higher temperature annealing at 800°C results in an increase in the channelled Ge (as well as the Si yield in the SiGe layer). We believe that this is due to the relaxation of the strained layer through the production of dislocations in the regrown layer at high temperature.

For the high dose sample, after complete SPE (600°C for 30 min.)  $\chi_{\min}(\text{Ge})$  is 19% (Fig. 3(b)). The high  $\chi_{\min}(\text{Ge})$  means that the regrown layer is a single crystal with high defect

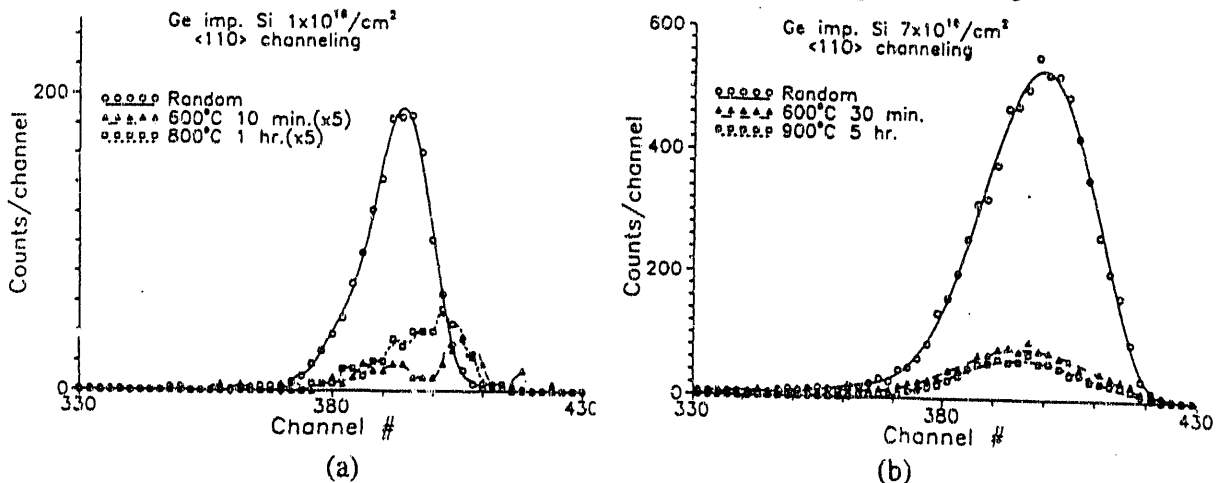


Fig. 3 The Ge signals from the random and <110> aligned RBS spectra of the (a) low dose, and (b) high dose samples annealed at various conditions.

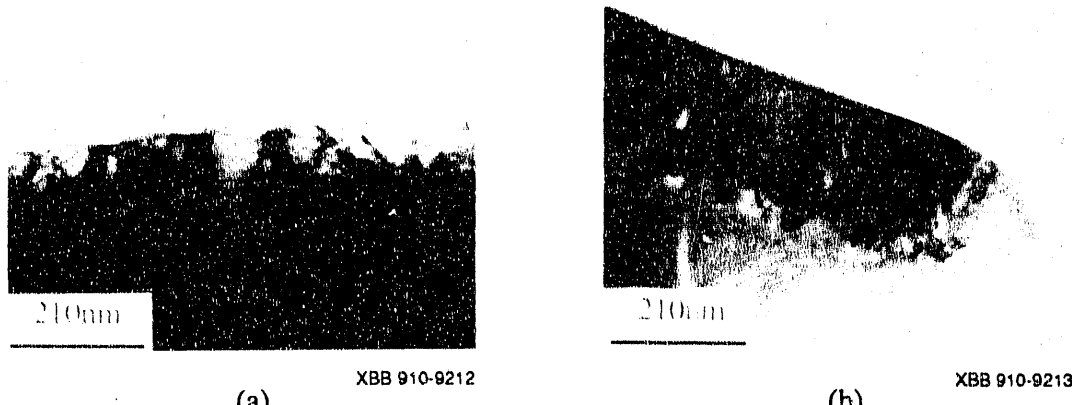


Fig. 4 Cross-sectional TEM micrographs of the high dose sample annealed at (a) 570°C for 25 min. and (b) 900°C for 1 hr.

density. Further annealing at 900°C for 5 hr. reduces the  $\chi_{\min}$  (Ge) to 15% indicating that there is an improvement in the crystallinity of the layer. Fig. 4 shows cross-sectional TEM micrographs of the high dose samples annealed at 570°C for 25 min. (a) and 900°C for 1 hr. (b). The sample annealed at 570°C is only partially regrown with the a/c interface near the peak of the Ge distribution. Fig. 4 clearly shows that the density of extended defects, namely threading dislocations and stacking faults in the regrown layer is reduced as the annealing temperature increases. Extended defects are still present in the  $\text{Si}_{1-x}\text{Ge}_x$  layer even after annealing at 900°C. These extended defects may be the result of high implant temperature (room temperature) [26] or strains due to the high Ge content in the layer. The random RBS spectra from the samples annealed at various temperatures show that the redistribution of Ge atoms in the layer even after 900°C annealing is not detectable.

The strains due to the lattice mismatch between the  $\text{Si}_{1-x}\text{Ge}_x$  layer and the substrate Si are accessed by ion channeling in the  $\langle 112 \rangle$  axis along a  $\{110\}$  planar direction. This orientation is chosen so as to minimize the channel steering effect [27,28]. The angular scans of the bulk Si and Ge signals for the fully regrown low dose sample (600°C for 10 min.) are plotted in Fig. 5. Since the layer is compositionally graded, a definite "kink" angle for ion channeling as is observed in sharp strained layers is not expected. Instead if the system is indeed strained an asymmetric broadened Ge scan should be observed. In Fig. 5 a best fit of the scans does not show any definite kink angle between the Si and Ge scans. However the broadened asymmetric Ge scan indicates that the layer is strained. Angular scans for similar samples after annealing at 800°C show only Ge scans similar to those of the bulk Si indicating that the layer after SPE is strained but becomes relaxed after high temperature annealing. Angular scans of the high dose sample after SPE as well as after high temperature annealing show no broadening in the Ge scans. From these channeling data we can conclude that graded  $\text{Si}_{1-x}\text{Ge}_x$  layers with peak Ge concentration around 4 atomic % are strained after SPE, but these strained layers become relaxed after annealing at temperatures higher than 800°C. This is also confirmed by the results shown in Fig. 3(a) which shows the presence of a higher defect density in the  $\text{Si}_{1-x}\text{Ge}_x$  layer annealed at 800°C due to strain relaxation. Regrown samples with Ge peak concentration at ~13 atomic %, however, are not strained. Robinson *et. al.* [29] studied the coherence of MBE grown  $\text{Si}_{1-x}\text{Ge}_x$  layers amorphized by implantation and then subjected to SPE at 600°C. They found that after SPE, layers with  $x < 18\%$  remain strained and the quality of layers with  $x > 18\%$  deteriorates as a function of  $x$ . Holländer *et. al.* [30] found

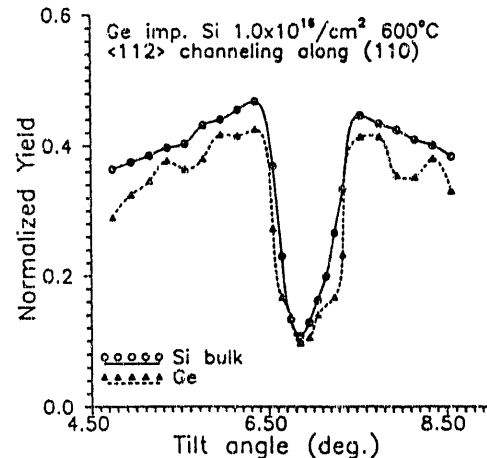


Fig. 5 Angular scans of the Ge from the  $\text{Si}_{1-x}\text{Ge}_x$  layer and the bulk Si signals across the  $\langle 112 \rangle$  axis parallel to a  $\{110\}$  plane for a low dose sample annealed at 600°C for 10 min.

quality of layers with  $x > 18\%$  deteriorates as a function of  $x$ . Holländer *et. al.* [30] found that annealing of  $\text{Si}_{1-x}\text{Ge}_x$  layers with  $x=20\%$  to above  $800^\circ\text{C}$  results in relaxation of the layers. Since our samples were implanted at room temperature to much higher ion doses (1-2 orders of magnitude) than those investigated by Robinson *et. al.*, more implantation induced defects due to defect coalescence during implantation are present. These defects may provide a means for the production of misfit dislocations in the layers. Therefore the critical Ge content for strained layers in our IBS samples is lower than those grown by MBE.

### III. Implantation Induced Defects

Fig. 6 shows the Si signals of a series of RBS spectra taken in the  $\langle 111 \rangle$  direction from an unimplanted Si wafer and the medium dose sample annealed at  $600^\circ\text{C}$  10 min.,  $800^\circ\text{C}$  10 min. and  $900^\circ\text{C}$  1 hr. The peaks at around channel #240 correspond to the direct scattering of the beam from the end-of-range (E-O-R) defects just below the original amorphous/crystalline (a/c) interface. It was suggested that these E-O-R defects arise from the Si self interstitials due to recoils during the implantation process. These interstitials then condense into extra planes of atoms forming dislocation loops upon annealing [31,32].

In Fig. 6, we notice that the intensity of the E-O-R peak decreases as the annealing temperature increases. After annealing at  $900^\circ\text{C}$  for 1 hr. the E-O-R peak is reduced by more than a factor of two. Maher *et. al.* [26] have studied the annealing of implantation induced defects and observed the coarsening of the E-O-R defects into resolvable a/c dislocation loops for self implanted Si to a dose of  $10^{14}$ - $10^{15}/\text{cm}^2$  after rapid thermal annealing at  $1200^\circ\text{C}$  for 5 seconds. The coarsening of the E-O-R defects after high temperature annealing is also observed in Fig. 4.

The extent of the E-O-R defects in the samples with the different doses annealed at  $900^\circ\text{C}$  is shown in Fig. 7. Note that in the high dose sample not only the intensity of the E-O-R defects is much higher, the dechanneling rate in region of channel # 250-270 corresponding to the original amorphous layer region (also the  $\text{Si}_{1-x}\text{Ge}_x$  region) is very high. This high dechanneling rate indicates a high density of defects present in this region consistent with the findings in the previous section from the values of the  $\chi_{\min}$  (Ge), and is confirmed by the cross-sectional TEM micrograph shown in Fig. 4.

## SUMMARY

We have studied the formation of buried epitaxial  $\text{Si}_{1-x}\text{Ge}_x$  layers in (100) Si by the IBS technique. Strained defect-free  $\text{Si}_{1-x}\text{Ge}_x$  layers with maximum  $x \sim 0.04$  was synthesized by implanting  $1 \times 10^{16}$  Ge ions/ $\text{cm}^2$  into Si at room temperature and annealed at  $600^\circ\text{C}$  for 10 min. These strained layers become relaxed after annealing at temperatures higher than  $800^\circ\text{C}$ . High dose implantation ( $7 \times 10^{16}/\text{cm}^2$ ) and SPE results in the formation of a relaxed  $\text{Si}_{1-x}\text{Ge}_x$  layer (maximum  $x \sim 0.13$ ) with high defect density. The implantation induced defects, namely threading dislocations and stacking faults in the layers and the E-O-R defects below the a/c interface can be reduced by annealing at temperatures higher than  $900^\circ\text{C}$ . No redistribution of the Ge atoms is detected even after annealing at  $900^\circ\text{C}$  for 5 hrs.

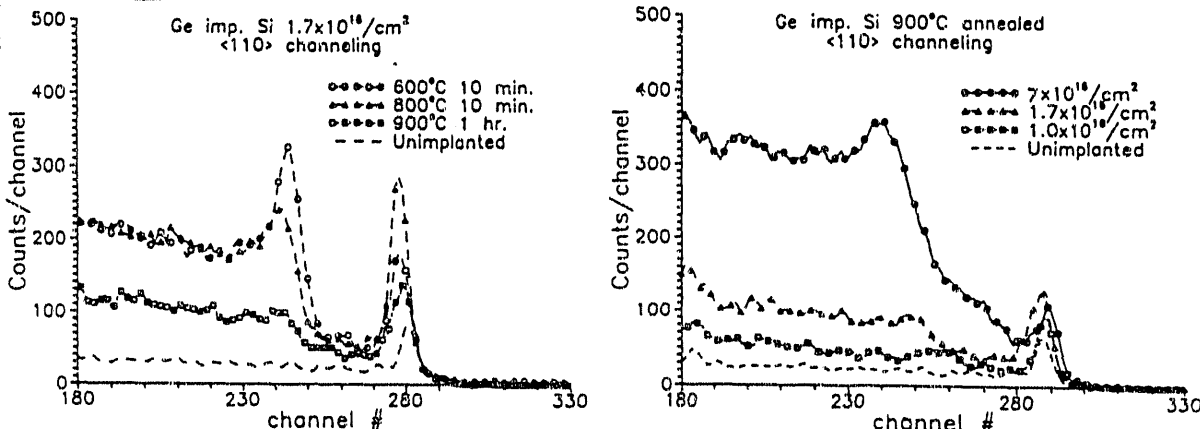


Fig. 6 A series of  $\langle 110 \rangle$  aligned RBS spectra from an unimplanted Si and medium dose samples annealed at various conditions.

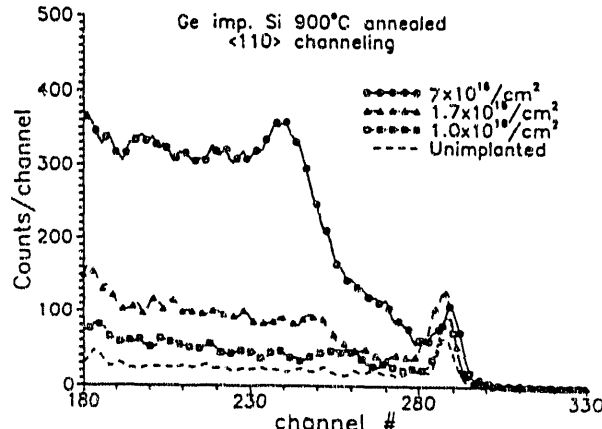


Fig. 7  $\langle 110 \rangle$  aligned RBS spectra of the samples with different Ge doses annealed at  $900^\circ\text{C}$ .

This work was supported by the Director, Office of Energy Research, Office of Basic Energy Sciences, Materials Science Division of the U. S. Department of Energy under Contract No. DE-AC03-76SF00098.

## REFERENCES

1. G. Abstreiter, H. Brugger, T. Wolff, H. Jorke, and H. J. Herzog, *Phys. Rev. Lett.* **54**, 2441 (1985).
2. S. S. Iyer, G. L. Patton, S. L. Delage, S. Tiwari, and J. M. C. Stork, *Proc. Symp. on Silicon Molecular Beam Epitaxy, Hawaii, 1987*, eds. J. C. Bean and L. J. Schowalter (The Electrochemical Soc. Inc.) p. 114.
3. J. C. Bean, T. T. Sheng, L. C. Feldman, A. T. Fiory, and R. T. Lynch, *Appl. Phys. Lett.* **44**, 102 (1984).
4. C. A. King, J. L. Hoyt, C. M. Grant, J. F. Gibbons, M. P. Scott, and T. Turner, *IEEE Electron. Dev. Lett.* **EDL-10**, 52 (1989).
5. F. Meyer, M. Zafrany, M. Eisenberg, R. Beserman, C. Schwebel, and C. Pellet, *J. Appl. Phys.* **70**, 4268, (1991).
6. J. W. Methews, *Epitaxial Growth*, ed., J. W. Methews (Academic Press, 1974) p.559.
7. R. Hull and J. C. Bean, *Mat. Res. Soc. Symp. Proc.* **148**, 309 (1989).
8. D. J. Howard, D. C. Paine, and N. G. Stoffel, *Mat. Res. Soc. Symp. Proc.* **187**, 279 (1991).
9. D. C. Paine, D. J. Howard, N. G. Stoffel, J. A. Horton, *J. Mater. Res.* **5**, 1023 (1990).
10. M. Berti, G. Mazzi, L. Calcagnile, A. V. Drigo, P. G. Merli, and A. Migliori, *J. Mater. Res.* **6**, 2120 (1991).
11. D. C. Paine, D. J. Howard, and N. G. Stoffel, *J. Electron. Mater.* **20**, 735 (1991).
12. A. White, K. T. Short, R. C. Dynes, J. P. Gorno, and J. M. Gibson, *Appl. Phys. Lett.* **50**, 95 (1987).
13. A. White, K. T. Short, R. C. Dynes, R. Hull, and S. M. Vandenberg, *Nucl. Instrum. Meth.* **B39**, 253 (1989).
14. S. Mantl, R. Jebasinski, and D. Hartman, *Nucl. Instrum. Meth.* **B59/60**, 666 (1991).
15. M. F. Wu, A. Vantomme, G. Langouche, H. Vanderstraeten, and Y. Bruynseraede, *Nucl. Instrum. Meth.* **B54**, 444 (1991).
16. R. S. Spraags, K. J. Reeson, R. M. Gwilliam, B. J. Sealy, A. DeVeirman, and J. vanLanduyt, *Nucl. Instrum. Meth.* **B55**, 836 (1991).
17. J. K. N. Lindner and E. H. teKaat, *J. Mater. Res.* **3**, 1238 (1988).
18. J. K. N. Lindner, T. Klassen, and E. H. teKaat, *Nucl. Instrum. Meth.* **B59/60**, 655 (1991).
19. K. M. Yu, B. Katz, and I. G. Brown, *Nucl. Instrum. Meth.* **B58**, 27 (1991).
20. F. Namavar, F. H. Sanchez, J. I/ Budnick, A. H. Fasihudin, and H. C. Hayden, *Mat. Res. Soc. Spring Meeting, 1987, Symp. C, Anaheim, CA.*
21. T. L. Alford and J. C. Barbour, *Mat. Res. Soc. Symp. Proc.* **157**, 137 (1990).
22. I. G. Brown, M. R. Dickinson, J. E. Galvin, X. Godechot, and R. A. MacGill, *Nucl. Instrum. Meth.* **B55**, 506 (1991).
23. I. G. Brown, B. Feinberg, and J. E. Galvin, *J. Appl. Phys.* **63**, 4889 (1988).
24. G. L. Olson and J. A. Roth, *Mater. Sci. Reports* **3**, 1 (1988).
25. D. C. Paine, N. D. Evans, and N. G. Stoffel, *J. Appl. Phys.* **70**, 4278 (1991).
26. D. M. Maher, R. V. Knoell, M. B. Ellington, and D. C. Jacobson, *Mat. Res. Soc. Symp. Proc.* **52**, 93 (1986).
27. R. Flagmeyer and M. Hörlecke, *Nucl. Instrum. Meth.* **B30**, 219 (1988).
28. Kin Man Yu and K. T. Chan, *Appl. Phys. Lett.* **56**, 45 (1990).
29. B. J. Robinson, B. T. Chilton, P. Ferret, and D. A. Thompson, *Mat. Res. Soc. Symp. Proc.* **160**, 353 (1989).
30. B. Holländer, S. Mantl, B. Stritzker, H. Jorke, and E. Kasper, *J. Mater. Res.* **4**, 163 (1989).
31. J. Thornton, P. L. E. Hemment, and I. H. Wilson, *Nucl. Instrum. Meth.* **B19/20**, 307 (1987).
32. J. Thornton, K. C. Paus, R. P. Webb, I. H. Wilson, and G. R. Booker, *J. Phys. D: Appl. Phys.* **21**, 334 (1988).

END

DATE  
FILMED

8 / 26 / 92

